Neuron, Vol. 17, 1231–1240, December, 1996, Copyright ©1996 by Cell Press

Synaptic Currents Generated by Neuronal Acetylcholine Receptors Sensitive to α-Bungarotoxin

Zhong-wei Zhang,* Jay S. Coggan, and Darwin K. Berg
Department of Biology
University of California, San Diego
La Jolla, California 92093-0357

Summary

Nicotinic acetylcholine receptors are widely distributed throughout the nervous system, but their functions remain largely unknown. One of the most abundant is a class of receptors that contains the α7 gene product, has a high relative permeability to calcium, and binds α-bungarotoxin. Here, we report that receptors sensitive to α-bungarotoxin, though concentrated in perisynaptic clusters on neurons, can generate a large amount of the synaptic current. Residual currents through other nicotinic receptors are sufficient to elicit action potentials, but with slower rise times. This demonstrates a postsynaptic response for α-bungarotoxin-sensitive receptors on neurons and suggests that the functional domain of the postsynaptic membrane is broader than previously recognized.

Introduction

Nicotinic acetylcholine receptors (AChRs) are cation-selective, ligand-gated ion channels that are widely distributed in the nervous system (Sargent, 1993). A wealth of behavioral studies implicate neuronal AChRs in central nervous system (CNS) function including state of arousal, level of attention, and short-term memory formation (Clarke et al., 1995). The potency of nicotine addiction testifies to the impact of AChRs on motivational pathways. Changes in the number and distribution of neuronal AChRs accompany several cognitive disorders and pathological conditions including Alzheimer's disease and Parkinson's disease. Gene knockout experiments with transgenic mice show that loss of a gene encoding a single neuronal AChR subunit can produce subtle deficits in associative memory (Picciotto et al., 1995).

Despite their participation in broad behavioral phenomena, little is known about how neuronal AChRs achieve their effects. Their similarities to AChRs at the neuromuscular junction led to the common expectation that neuronal AChRs would have a postsynaptic location and mediate fast, excitatory synaptic transmission. With a few notable exceptions, however, excitatory nicotinic transmission has been difficult to document in the nervous system. Instead, evidence has accumulated indicating that neuronal AChRs may act at presynaptic sites to enhance neurotransmitter release and thereby modulate synaptic transmission (McGehee and Role, 1995).

One of the most prominent classes of neuronal AChRs both in the CNS and in the peripheral nervous system (PNS) contains the α7 gene product. Such receptors have a high relative permeability to calcium and bind α-bungarotoxin (αBgt) with high affinity (Couturier et al., 1990; Schoepfer et al., 1990; Bertrand et al., 1993; Seguela et al., 1993). Activation of the receptors can produce a rapidly decaying inward current (Zorumski et al., 1992; Alkondon and Albuquerque, 1993; Zhang et al., 1994) and can quickly elevate intracellular levels of free calcium in neurons (Vijayaraghavan et al., 1992). In cell culture, the receptors have been shown to activate calcium-dependent processes including neurite retraction (Pugh and Berg, 1994) and release of arachidonic acid (Vijayaraghavan et al., 1995). A recent report indicates that AChRs containing the α7 gene product act at presynaptic sites to modulate synaptic transmission by enhancing release of both glutamate and ACh (McGehee et al., 1995). No evidence to date has suggested a postsynaptic role for α7-containing receptors.

Large numbers of AChRs containing the α7 gene product and capable of high affinity αBgt binding are found on chick ciliary ganglion neurons (Chiappinelli and Giacobini, 1978; Smith et al., 1985; Vernallis et al., 1993). The receptors are undetectable in synaptic membrane on the neurons identified by ultrastructural criteria and appear instead at extrasynaptic sites (Jacob and Berg, 1983; Loring et al., 1985). Confocal immunofluorescent imaging suggests the receptors are concentrated in perisynaptic clusters on the neurons (Wilson Horch and Sargent, 1995). This is true both for ciliary neurons in the ganglion that innervate striated muscle in the iris and ciliary body and for choroid neurons in the ganglion that innervate smooth muscle in the vasculature of the choroid layer. The reported perisynaptic distribution persists in the adult, indicating that it is not a developmentally transient phenomenon.

Early electrophysiological analysis using extracellular recording to monitor compound action potentials suggested the receptors were not necessary for synaptic transmission. Incubating whole ciliary ganglia in αBgt did not prevent preganglionic stimulation from eliciting action potentials in the postganglionic nerve root (Chiappinelli et al., 1981; Chiappinelli, 1985). Other classes of AChRs, notably those concentrated in part at postsynaptic densities (Jacob et al., 1984; Halvorsen and Berg, 1987; Loring and Zigmond, 1987), were thought responsible for synaptic transmission through the ganglion (Chiappinelli et al., 1981; Loring et al., 1984).

We have recorded from neurons in whole ganglia using the whole-cell patch-clamp configuration to measure directly the contributions of αBgt-sensitive and αBgt-insensitive AChRs to the evoked synaptic current. We have also examined spontaneous synaptic currents in the neurons to determine which receptor classes are responsible for them, and have used intracellular recording to examine the action potentials produced by receptor activation. We show here that αBgt-sensitive receptors produce a large fraction of the synaptic current despite an apparent perisynaptic location.

*Present address: Centre de Recherche en Neurobiologie, Université Laval, l'Hôpital de l'Enfant-Jesus, Quebec G1J 1Z4, Canada.

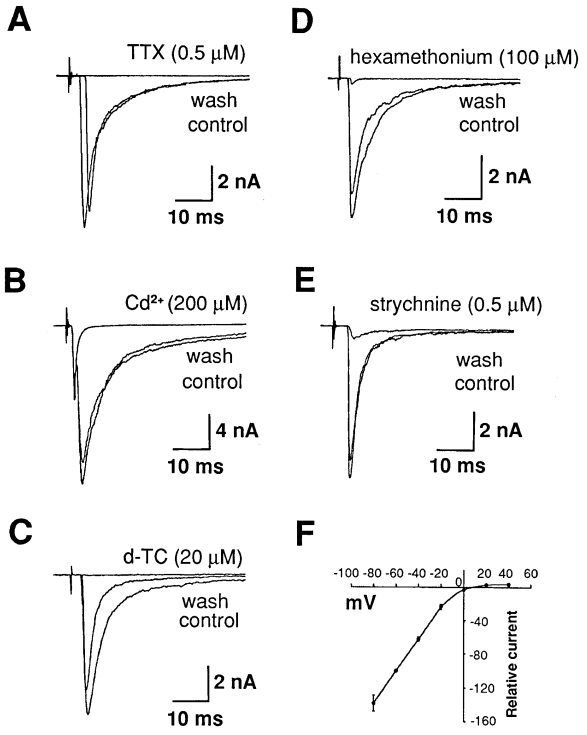

Figure 1. Properties of Evoked Synaptic Currents Recorded from Neurons in Intact Chick Ciliary Ganglia

In (A)–(E), superimposed traces of evoked synaptic currents are shown for a neuron before (control), during (drug), and after (wash) exposure to the indicated drug. Holding potentials were −70 mV unless otherwise indicated.

(A) TTX at 0.5 μM; 1 min wash to remove. The lengthened synaptic delay observed after the wash resulted from a residual presynaptic TTX blockade; subsequent washing reduced the delay to control values.

(B) Cd^{2+} at 200 μM; 3 min wash to remove. The small inward current preceding the evoked synaptic current is most likely the result of electrical coupling between the pre- and postsynaptic elements passing current from the presynaptic action potential.

(C) d-TC at 20 μM; 6 min wash.

(D) Hexamethonium at 100 μM; 2 min wash.

(E) Strychnine at 0.5 μM; 2 min wash.

(F) Steady-state I–V curve of evoked synaptic currents. Peak currents obtained at the indicated holding potentials were normalized to those obtained at −60 mV (which were given a value of −100) in the same cell. Each point represents mean ± SEM of values obtained from four to five cells.

Results

Evoked Synaptic Currents

Synaptic currents were recorded from chick ciliary ganglion neurons in situ using the whole-cell patch-clamp configuration under voltage clamp. No effort was made to distinguish ciliary from choroid neurons. The currents were evoked by stimulating the presynaptic oculomotor nerve root with a suction electrode. Fast inward currents were detected after a delay of 2–4 ms following the stimulus artifact. Current amplitudes fell between 2 and 8 nA in most cases; little variation was seen over repeated trials in the same neuron. Tetrodotoxin (TTX) at 0.5 μM reversibly blocked the currents as expected for synaptic responses evoked by action potentials elicited in the presynaptic nerve (Figure 1A; n = 3 cells). Similarly, the responses were reversibly blocked by 200 μM Cd^{2+}, which inhibits voltage-gated calcium channels and thereby prevents calcium-dependent neurotransmitter release (Figure 1B; n = 5). In some cases, a small current preceded the large synaptic current and was reminiscent of a presynaptic action potential (Figure 1B); such currents were unaffected by 200 μM Cd^{2+} and presumably resulted from the electrical coupling that can occur between a ciliary neuron and its presynaptic nerve terminal (Martin and Pilar, 1964; Dryer and Chiappinelli, 1985).

The evoked synaptic currents had a mean rise time of 0.67 ± 0.03 ms (mean ± SEM, n = 23 cells), measured as the time required for the current to rise from 10% to 90% of peak value. The decay phase of the currents could be fit by the sum of two exponentials having time constants of 2.3 ± 0.2 and 23.9 ± 1.8 ms (n = 23 cells). For the majority of cells, the amplitude of the evoked current was stable throughout the recording period (20–60 min).

αBgt Blockade

Consistent with previous findings (Yawo and Chuhma, 1994), the evoked synaptic currents displayed a nicotinic cholinergic pharmacology. They were blocked reversibly by 20 μM d-tubocurarine (d-TC; Figure 1C; n = 4) and by 100 μM hexamethonium (Figure 1D; n = 7). Strychnine, a classic antagonist of glycine receptors, at 1 μM inhibits α7-containing receptors expressed in Xenopus oocytes (Seguela et al., 1993) and nicotinic receptors sensitive to αBgt in ciliary ganglion neurons (Zhang et al., 1994). At 0.5 μM, strychnine reversibly blocked the evoked synaptic currents (Figure 1E; n = 4). The currents reversed at about 0 mV and showed a strong inward rectification at positive membrane potential (Figure 1F) as reported for all neuronal nicotinic receptors previously tested (Sargent, 1993; McGehee and Role, 1995).

The evoked synaptic currents were markedly inhibited by 50 nM αBgt (Figure 2A; n = 6 cells). Unlike d-TC and hexamethonium, the effect of αBgt appeared slowly and reached a maximum after 2–3 min of application (Figure 2B). The blockade by αBgt persisted even after 30 min of rinsing, suggesting high affinity binding of the toxin. Similar results were obtained with 25 nM αBgt (n = 3 cells), though the time to maximum blockade was slightly longer. Combining the results showed that αBgt inhibited the mean peak current amplitude by 92.0% ± 0.7% (n = 9 cells). The total amount of charge carried by the synaptic current was determined by integrating under the current records over a 50 ms period starting with the onset of the evoked response. Comparing the values obtained in the presence and absence of toxin indicated that 49.1% ± 4.0% (mean ± SEM; n = 9 cells) of the charge entering the cell during the evoked response was carried by the αBgt-sensitive synaptic current. Analyzing the time course of the evoked response indicated that αBgt completely abolished the rapidly decaying component and slightly increased the decay constant of the slow component (Table 1).

Access of Neurotransmitter

The finding that αBgt-sensitive AChRs rapidly generate a large fraction of the synaptic current was unexpected

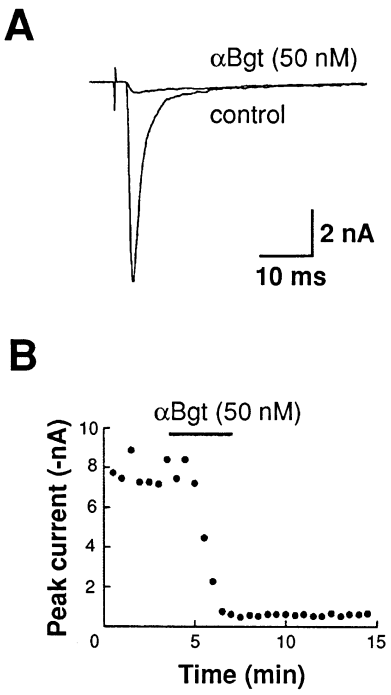

Figure 2. Effect of αBgt on Evoked Synaptic Currents

(A) Superimposed current traces showing evoked responses before (control) and after (αBgt) a 3 min incubation with 50 nM αBgt.

(B) Time course of αBgt blockade. Synaptic currents were evoked every 30 s in the presence and absence of αBgt. The horizontal bar indicates the period when αBgt was present. αBgt completely abolished the fast component of the synaptic current. The blockade was irreversible over the time period examined.

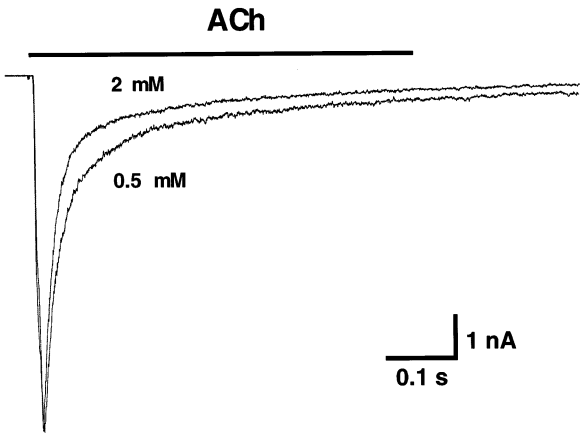

Figure 3. ACh Responses from Isolated Neurons

Two superimposed traces are shown from the same cell, indicating the whole-cell current elicited by 0.5 and 2 mM ACh applied from a large bore pipette at 2 min intervals. The neuron was freshly dissociated from an E14 chick ciliary ganglion. Calibration bars: horizontal, 0.1 s; vertical, 1 nA. Long horizontal line: duration of ACh application; holding potential, −60 mV.

in view of the reported perisynaptic location of the receptors on ciliary ganglion neurons. One possibility was that the toxin-sensitive currents were generated by previously undetected αBgt-sensitive AChRs concentrated in conventional postsynaptic membrane on the neurons, i.e., that demarcated by a straightening and thickening of the postsynaptic membrane immediately juxtaposed to presumed presynaptic sites of vesicle release (Jacob and Berg, 1983). Quantitative autoradiography at the ultrastructural level sets an upper limit on such receptors as being no more than a few percent at most of the total number of αBgt-sensitive AChRs present (Loring and Zigmond, 1987). To assess the likelihood that a few percent of the αBgt-sensitive receptors on the cells could account for the observed αBgt-sensitive synaptic currents, we compared the magnitude of the currents with that of the maximum whole-cell ACh response from dissociated neurons.

ACh was applied to isolated neurons using a fast delivery system (Figure 3). This procedure activates both the rapidly decaying αBgt-sensitive response and the more slowly decaying αBgt-resistant response (Zhang et al., 1994). Mean peak responses of 9.9 ± 1.2 and 9.1 ± 1.0 nA (mean ± SEM; n = 15 and 22 cells) were elicited with 0.5 and 2 mM ACh, respectively. The lower concentration was sufficient to induce a maximal response under the conditions used. Correcting the current amplitudes for differences in holding potentials (−60 versus −70 mV) indicated that the mean peak synaptic current observed in situ was nearly half as great as the maximal whole-cell ACh response that could be elicited from dissociated neurons. Since over 90% of the peak synaptic current in situ arises from αBgt-sensitive AChRs, the comparison does not support the hypothesis that the current is generated by a few αBgt-sensitive receptors that previously escaped detection in the specialized postsynaptic membrane on the cells (Jacob and Berg, 1983; Loring and Zigmond, 1987; Wilson Horch and Sargent, 1995).

Table 1. Effects of αBgt on Properties of Evoked Synaptic Currents

Treatment	Peak Current (−nA)	Rise Time (ms)	Decay Times (ms)
Before αBgt (n = 9)	5.14 ± 0.92[b]	0.61 ± 0.03[c]	1.84 ± 0.14 20.42 ± 3.31[d]
After αBgt (n = 9[a])	0.39 ± 0.08[b]	1.45 ± 0.25[c]	27.25 ± 4.34[d]

Whole-cell patch-clamp recording was used to measure the indicated properties of synaptic currents evoked in ciliary ganglion neurons by stimulation of the oculomotor nerve root before and after treatment with αBgt. Values represent the mean ± SEM of the number of cells indicated by n.

[a] Data from six cells treated with 50 nM αBgt and three cells treated with 25 nM were combined, since no significant difference was found between them.

[b] $p \leq 0.001$ by paired t test.

[c] $p \leq 0.02$ by paired t test.

[d] $p \leq 0.02$ by paired t test.

More detailed comparisons between the synaptic currents in the ganglion and the ACh responses in vitro are complicated by their differences in kinetics. The rapidly decaying component of the response elicited by 2 mM ACh in vitro has a rise time of 8.6 ± 0.9 ms (mean ± SEM; n = 21 cells) and a time constant of decay of 28.3 ± 2.8 ms (n = 21). These are an order of magnitude slower than those of the rapidly decaying synaptic current in the ganglion. Responses elicited by 0.5 mM ACh have an even slower time constant of decay for the fast component (40.1 ± 4.8 ms; n = 15; $p \leq 0.04$ by unpaired t test), though the rise time (9.6 ± 1.2 ms; n = 15) is comparable to that evoked by 2 mM ACh. Receptor desensitization is known to depend on agonist concentration. The method of application may also be a contributing factor. If receptor activation is spread over a greater period of time because of delays in transmitter reaching all sides of the cell (consistent with the slow rise times), a corresponding spread in receptor inactivation would be expected. As a result, a comparison of peak amplitudes should be considered only a first approximation; the number of openings per receptor may differ in the two test situations.

Effects of an Acetylcholinesterase Inhibitor

A different approach to assessing the location of AChR populations activated in situ is to examine the effects of an acetylcholinesterase (AChase) inhibitor. The ganglion contains high levels of AChase activity that are likely to terminate transmitter action following release from presynaptic sites (Scarsella et al., 1978; Couraud et al., 1980; Kato et al., 1980; Olivieri-Sangiacomo et al., 1983). Using an AChase inhibitor to extend the lifetime of released ACh should permit the transmitter a greater radius of diffusion. If only a small fraction of the αBgt-sensitive AChRs are normally reached by transmitter (e.g., those receptors in the immediate postsynaptic membrane), increasing the radius of transmitter diffusion may access the abundant perisynaptic receptors and dramatically extend the αBgt-sensitive synaptic current. This was tested by comparing the decay times of synaptic currents before and after exposure of ganglia with phospholine, a potent AChase inhibitor.

Phospholine at 2 μM over a 10 min period had no significant effect on the rapidly decaying synaptic current, but did prolong the slowly decaying synaptic current (Figure 4A). Decay constants of 1.7 ± 0.2 and 1.4 ± 0.2 ms (mean ± SEM; n = 4 cells) were calculated for the rapidly decaying component before and after exposure to phospholine; the difference was not significant ($p \leq 0.15$ by paired t test). The slowly decaying component had mean decay times of 16.8 ± 1.8 and 40.3 ± 4.3 ms (n = 6 cells) before and after phospholine treatment, respectively; the increase was highly significant ($p \leq 0.005$). Synaptic stimulation of the same neuron at 30 s intervals throughout the phospholine treatment indicated that a 5 min exposure to phospholine was sufficient to produce the maximum effect on decay time (data not shown). Repeating the experiment on other cells after blockade of αBgt-sensitive AChRs showed that the slowly decaying component affected by phospholine treatment was αBgt-resistant as expected (Figure 4B). In the presence of αBgt, mean decay times of 10.0 ± 2.1 and 34.7 ± 2.6 ms (n = 3 cells; $p \leq 0.02$) were obtained for the slowly decaying component before and after treatment with phospholine, respectively.

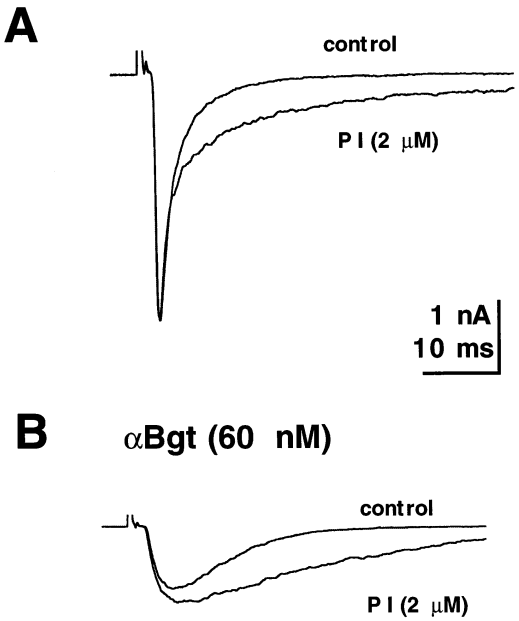

Figure 4. Effects of the AChase Inhibitor Phospholine on the Synaptic Currents

(A) Two superimposed traces from a cell showing the stimulus-evoked whole-cell synaptic currents recorded before (control) and after a 5 min exposure to 2 μM phospholine (PI).

(B) Two superimposed traces from a cell showing the whole-cell synaptic currents recorded in the presence of 60 nM αBgt before (control) and after (PI) the same phospholine exposure. Synaptic currents were evoked at 20 s intervals; holding potential, −60 mV.

The fact that the rapidly decaying component was not extended in duration by the phospholine treatment indicates that few additional αBgt-sensitive AChRs can be accessed by increasing the time of transmitter diffusion. Apparently the αBgt-sensitive synaptic current terminates because of receptor desensitization rather than transmitter hydrolysis. The prolonged current from αBgt-resistant AChRs in the presence of phospholine confirms the effectiveness of the AChase inhibitor. Phospholine, under the conditions used, had no direct effect on AChRs: perfusing dissociated neurons with 2 μM phospholine for 3–10 min produced no change in either the peak amplitude or the decay phase of the response elicited by ACh (data not shown).

Spontaneous Miniature Synaptic Currents

In some cases, spontaneous miniature synaptic currents were detected in the neurons (Figure 5A). The amplitudes varied over a considerable range with some events being barely detectable, while others were as great as 80 pA above baseline (Figure 5B). Treatment with 50 nM αBgt reduced the mean peak amplitude of the spontaneous events 4-fold in the example shown (Figure 5C). Comparing the mean peak amplitude of spontaneous events before and after αBgt treatment in two other cells yielded toxin-induced reductions of 2- and 3-fold. The actual reduction is likely to be even

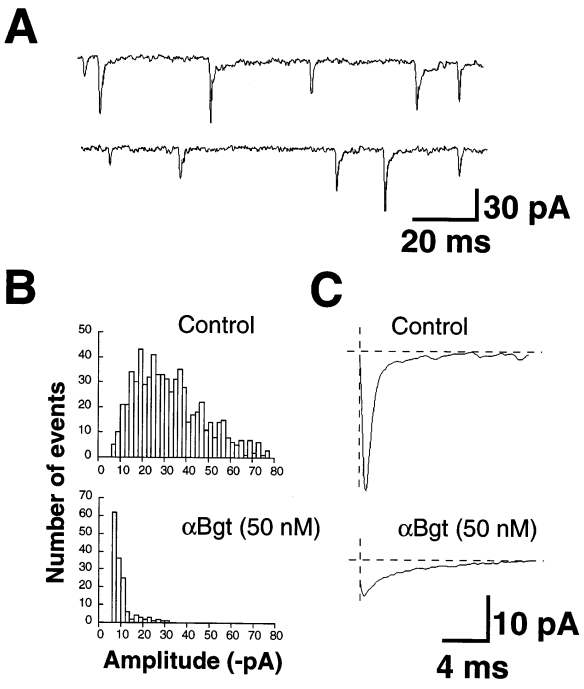

Figure 5. Effect of αBgt on Spontaneous Miniature Synaptic Currents

(A) Typical spontaneous current events recorded in a cell held at −60 mV.

(B) Amplitude histograms of spontaneous miniature synaptic currents recorded from the neuron for a 2 min period before (top) or for a 3 min period after perfusion with 50 nM αBgt (bottom) and grouped in bins of 2 pA. Prior to application of the toxin, the frequency of detected events was 60 ± 6 per 10 s with an average amplitude of −33.5 ± 0.7 pA. In the presence of 50 nM αBgt, the frequency of detected events was 7 ± 1 per 10 s with an average amplitude of −8.4 ± 0.4 pA.

(C) Average of consecutive synaptic events in the cell before (top; 146 events) and after (bottom; 143 events) incubation with 50 nM αBgt. Horizontal dashed lines indicate the baseline level. Events were aligned for averaging at the point immediately following the detected threshold point (vertical dashed lines). For spontaneous miniature currents in the absence of αBgt, the average amplitude was −30.4 pA with a decay constant of 1.0 ms. In the presence of αBgt, the average amplitude was −8.4 pA with a decay constant of about 6 ms. The threshold of detection was set at −6.5 pA for the cell.

greater because many of the smaller spontaneous events occurring in αBgt-treated cells would have been lost in the noise and therefore not properly weighted in calculating the average size observed after toxin treatment. As in the case of the evoked response, the blockade by αBgt was not reversible. The spontaneous events were resistant to 1 μM TTX, confirming the fact that they were not dependent on presynaptic action potentials.

The frequency of the spontaneous events in the absence of αBgt varied greatly from cell to cell and did not correlate with the size of the evoked response. In several cases, a sufficient number of spontaneous events (200–500) was obtained from a single cell to permit calculation of a mean response that could be analyzed for its rate of decay. Fitting the decay phase required the sum of two exponentials for each cell and yielded time constants of 0.7 ± 0.2 and 11 ± 5 ms (mean ± SEM; n = 4 cells), respectively. These values are in reasonable agreement with those describing the rapidly and slowly decaying components, respectively, of the evoked response. The mean peak amplitude of the spontaneous events in the four cells, obtained by averaging the four individual means, was 36 ± 5 pA. A similar analysis of decay times in the presence of αBgt could not be carried out because the spontaneous events were smaller and yielded a less favorable signal-to-noise ratio. Also, the frequency of spontaneous events in the presence of αBgt appeared much reduced (Figure 5B). If toxin blocks the rapidly decaying component of the spontaneous events as it does the rapidly decaying component of the evoked responses, it would account for the reduction in amplitude reported above and would cause many of the events to go undetected because of their small size. This could easily explain the decreased frequency of spontaneous events following αBgt treatment.

Synaptic Stimulation of Action Potentials

Intracellular recording was used to determine whether the small synaptic currents remaining in the presence of αBgt were sufficient to elicit action potentials in the neurons. Incubating the intact ganglion in 100 nM αBgt for more than an hour did not alter the resting potential or change the threshold for firing action potentials in response to depolarizing current pulses (Figures 6A and 6B). Nor did it affect the input resistance, time constant, or mean height of evoked action potentials in the neurons (Table 2). Most important, the αBgt treatment did not prevent the neurons from firing an action potential in response to synaptic input elicited by stimulation of the presynaptic nerve root (Figures 6C and 6D). The only detectable effect of the αBgt treatment on the neurons under these conditions was a broadening of the rising phase of the action potential (Figures 6C and 6D; Table 2). In contrast, incubation with 40 μM d-TC for 5 min completely blocked the ability of presynaptic stimulation to elicit action potentials (n = 3 cells; data not shown). In no case were multiple action potentials triggered in the ganglionic neuron by the single brief stimulation of the presynaptic nerve root used here. The results demonstrate that currents through αBgt-insensitive AChRs on the neurons are sufficient to elicit an action potential in situ. αBgt-sensitive receptors, by virtue of their ability to produce large and rapid depolarizations, shorten the time to threshold for triggering the action potential, and thereby give the appearance of decreasing its rise time.

Discussion

The principal findings reported here are that αBgt-sensitive AChRs rapidly generate over 90% of the peak synaptic current in ciliary ganglion neurons and apparently do so from a predominantly perisynaptic location. Though the receptors are known to be widely distributed throughout both the CNS and PNS, we could find no previous demonstration of a postsynaptic role for αBgt-sensitive receptors on vertebrate neurons. The absence of the receptors from conventional postsynaptic specializations identified earlier on the neurons raises questions about the full extent of the functional synaptic

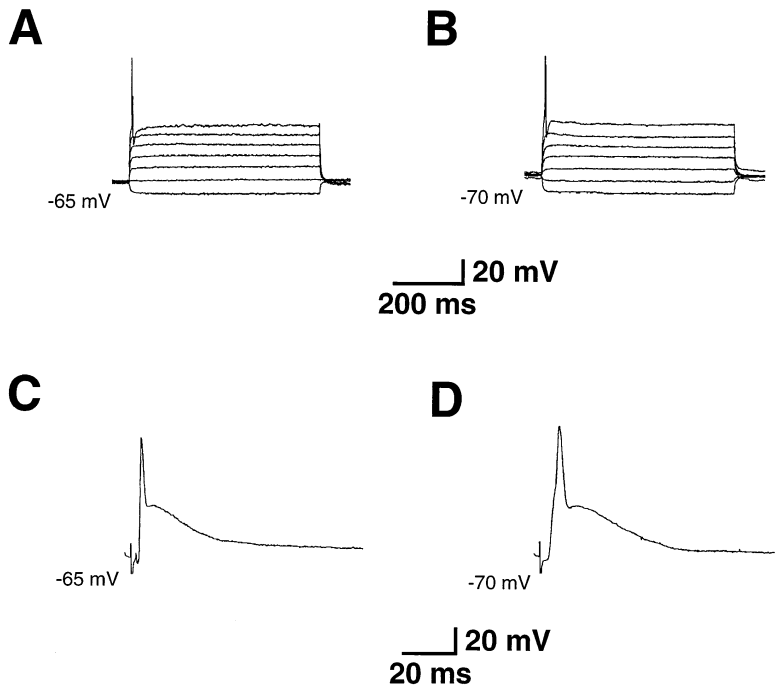

Figure 6. Effect of αBgt on the Ability of Synaptic Stimulation to Elicit Action Potentials

(A) Membrane properties revealed by constant current pulses (600 ms duration; 60 pA increments) applied intracellularly to a control neuron with a resting potential of −65 mV. Input resistance, 156 MΩ; time constant, 9.1 ms; threshold for action potentials, −25 mV.

(B) Membrane properties of a cell treated with αBgt (100 nM). Input resistance, 129 MΩ; time constant, 4.3 ms; threshold for action potentials, −26 mV.

(C) Membrane potential and action potential in the same cell as in (A) following stimulation of the oculomotor nerve (70 V, 40 μs). Height of the evoked action potential, 86 mV; rise time (10% to 90% of peak amplitude), 0.8 ms. The stimulation artifact was reduced for illustration.

(D) Synaptic events in the same cell as in (B) induced by stimulation of the oculomotor nerve (60 V, 25 μs) in 100 nM αBgt. Height of evoked action potential, 94 mV; rise time, 3.5 ms.

domain and the distance over which transmitter diffuses when released from presynaptic sites.

A recent report has shown that an αBgt-sensitive AChR can modulate transmitter release from presynaptic terminals (McGehee et al., 1995). It is clear that the toxin blockade of synaptic currents in the present case arises from αBgt-sensitive receptors on the postsynaptic neuron rather than from presynaptic receptors. αBgt completely blocks the fast component of the synaptic response evoked by nerve stimulation, while having little impact on the slow component. In addition, αBgt treatment reduces the mean amplitude of the spontaneous miniature synaptic currents. The spontaneous currents contain both fast and slow component prior to toxin treatment, and it is most likely the fast component that is blocked by the toxin; the small signal-to-noise ratio of the spontaneous events after toxin treatment did not permit a reliable quantitative analysis of the decay rates. The apparent decrease in frequency of the spontaneous events after αBgt treatment could arise either from a separate presynaptic effect of the toxin or from the reduced mean amplitude of the events causing many of them to be lost in the noise.

The αBgt-sensitive component of the synaptic current has the properties expected for responses from AChRs containing the α7 gene product on the neurons. It is fully blocked by nanomolar concentrations of αBgt within minutes, and the blockade is relatively irreversible as is true of αBgt binding to the receptors (Chiappinelli and Giacobini, 1978; Ravdin et al., 1981; Smith et al., 1985; Vernallis et al., 1993). (A previous report that certain commercial lots of αBgt blocked nicotinic transmission through the ciliary ganglion used micromolar concentrations of the toxin and resulted from a contaminant, κ-bungarotoxin, being present; the contaminant would have blocked both αBgt-sensitive and αBgt-insensitive AChRs [Chiappinelli and Zigmond, 1978; Chiappinelli et al., 1981].) Both the αBgt-sensitive component of the synaptic current measured here and that attributed to AChRs containing the α7 gene product on the dissoci-

Table 2. Effects of αBgt on Membrane Properties and Synaptic Potentials in Neurons

Treatment	Resting Potential (mV)	Input Resistance (MΩ)	Time Constant (ms)	Threshold for AP (mV)	Evoked AP Height (mV)	Evoked AP Rise Time (ms)
Control	−69 ± 2 n = 7	110 ± 15 n = 5	6.1 ± 1.1 n = 5	−24 ± 3 n = 5	84 ± 5 n = 6	1.38 ± 0.36[a] n = 6
αBgt (100 nM)	−69 ± 2 n = 6	121 ± 5 n = 5	4.9 ± 0.8 n = 5	−25 ± 1 n = 5	82 ± 4 n = 5	2.72 ± 0.45[a] n = 5

Intracellular recording was used to measure the indicated properties of ciliary ganglion neurons in the presence and absence of 100 nM αBgt. Values represent the mean ± SEM for the number of cells indicated by n. The input resistances and time constants were determined by measuring the membrane potential changes induced by hyperpolarizing current pulses. The threshold for initiation of action potentials (APs) was determined with a series of depolarizing current pulses. Evoked AP height was calculated as the difference between the resting potential and the peak of the AP. The AP rise time was measured as the time between 10% and 90% of the peak value of the depolarization.

[a]Significant difference ($p \leq 0.04$) determined by unpaired t test.

ated neurons (Zhang et al., 1994) are reversibly blocked by low concentrations of strychnine. Moreover, the peak amplitude of the αBgt-sensitive synaptic current is nearly half as large as the maximum αBgt-sensitive ACh response from freshly dissociated neurons. A minor species of membrane components capable of binding αBgt but lacking the α7 gene product has also been identified in ganglion extracts, but its location, subunit composition, and functional properties are unknown (Pugh et al., 1995).

The finding that αBgt-sensitive AChRs contribute much of the synaptic current was surprising in view of previous studies showing their absence from postsynaptic specializations on the neurons. Immunohistochemical staining at the electron microscopic level indicates that the receptors are instead localized in regions adjacent to postsynaptic membrane thickenings and are concentrated in the vicinity of short dendrites emanating from the cell bodies (Jacob and Berg, 1983). AChRs that bind other probes such as the monoclonal antibody (MAb) 35 but not αBgt can be found, in part, in the specialized postsynaptic membrane (Jacob et al., 1984; Loring and Zigmond, 1987). Similar conclusions were reached with confocal immunofluorescence that revealed clusters of αBgt-binding AChRs in perisynaptic locations, near but distinct from sites of transmitter release; no αBgt staining was apparent immediately under sites of transmitter release defined by the presence of a synaptic vesicle antigen (Wilson Horch and Sargent, 1995).

Are the so-called perisynaptic receptors contributing to the synaptic currents? The relatively large size of the αBgt-sensitive synaptic current suggests that they are. In fact, the ratio of the peak αBgt-sensitive and αBgt-insensitive synaptic currents is roughly comparable to the ratio of AChRs that do and do not bind αBgt in the ganglion (Chiappinelli and Giacobini, 1978; Smith et al., 1985; Vernallis et al., 1993). Moreover, the phospholine experiments demonstrate that few, if any, additional αBgt-sensitive AChRs can be reached by transmitter in situ when the time of diffusion is extended by blocking ACh hydrolysis. This would be expected if the perisynaptic αBgt-sensitive AChRs are normally being exposed to transmitter during synaptic stimulation even in the absence of the AChase inhibitor. The fact that the phospholine treatment extends the duration of the αBgt-resistant synaptic current demonstrates that the AChase inhibitor is effective. In other systems, even a 1 min exposure of 1 μM phospholine is sufficient to block 99% of the AChase activity (Radic et al., 1995). The increased duration of the αBgt-resistant current by phospholine could be caused either by transmitter reaching more distant receptors or by repeated activation of the same receptors. The αBgt-resistant receptors are known to desensitize more slowly than the αBgt-sensitive ones (Zhang et al., 1994) and, therefore, may be capable of repeated activation.

A similar conclusion about the proportion of αBgt-sensitive receptors reached by transmitter in situ emerges from comparing the peak amplitude of synaptic currents in the ganglion with the maximum ACh response elicited in vitro. While this indicates that the synaptic currents are likely to involve more than a few percent of the total functional AChRs on the cells, a more exact comparison is complicated by the different time courses of the responses. The slower rise time and decay of the in vitro response are not unexpected, given the method of agonist application. The method allows solution exchange within 2 ms when measured with an open recording pipette with a tip diameter of about 1 μm, but longer times are required to exchange the solution around a 20 μm diameter cell (Zhang et al., 1994). Because of this and because receptor desensitization depends on agonist concentration, the number of times a given receptor opens during application of agonist to an isolated neuron may differ significantly from the number of times a receptor opens during synaptic stimulation in situ. This limits the range of the comparison.

It would not be surprising if immersing the entire cell body in transmitter as occurs with the dissociated neurons ultimately causes more total receptors to be activated than occurs with synaptic stimulation in situ. Autoradiographic studies suggest that a substantial portion of the αBgt-binding AChRs may be distributed broadly at low density over the entire cell body (Loring et al., 1985). Such receptors would probably be too sparse to detect by confocal immunofluorescence and therefore would not have contributed to the perisynaptic clusters described. They probably also would be too distant from sites of transmitter release to be activated by synaptic stimulation.

Is it possible that transmitter released from traditional presynaptic sites would have time to reach perisynaptic clusters and activate αBgt-sensitive AChRs within the time frame observed? The clusters are estimated to be 1–4 μm in diameter and can be surrounded by presumed sites of transmitter release (Wilson Horch and Sargent, 1995). For diffusion from a point source into three-dimensional space, $R = (6DT)^{1/2}$ where R is the radius of diffusion, T is time, and D is the diffusion coefficient. For molecules of the size of ACh, D has a value of about 8×10^{-6} cm^2/s (Atkins, 1986). With no barriers, ACh could radially diffuse about 1.8 μm in 0.7 ms, the approximate time during which the αBgt-sensitive synaptic current rises from 10% to 90% of peak value. If the receptors have an extremely rapid rate of activation, transmitter being released simultaneously from multiple sites ringing the receptor cluster might well access most sites within it. The number of transmitter molecules released at individual sites in the ganglion is not known, but a recent estimate suggests that as few as 2000 molecules being released from a point source at a typical synapse could produce a concentration as high as 10 μM at a radius of 2 μm within 0.5 ms (Clements, 1996). These calculations indicate the plausibility of perisynaptic αBgt-sensitive AChRs being activated by transmitter released from presynaptic terminals in the ganglion.

An alternative possibility is that the designation of αBgt-binding AChR clusters as being perisynaptic on the neurons is misleading. The short dendrites and AChR clusters on ciliary ganglion neurons may constitute specialized structures designed to expose transmitter broadly and rapidly to a large number of receptors. It would be of interest to determine the fine structure of cell contacts in the immediate vicinity of the receptor clusters. Distributed release sites yet to be identified

and overlapping membranes may facilitate transmitter delivery to locations that appear perisynaptic by conventional criteria. The fact that similar perisynaptic AChR clusters have been described on adult neurons in the CNS suggests that the phenomenon may be a general one (Ullian and Sargent, 1995).

Chick ciliary ganglion neurons form synapses on each other when grown in dissociated cell culture, and the synapses can be spontaneously active. A previous study found that αBgt was unable to block the spontaneous synaptic depolarizations recorded with intracellular recording (Margiotta and Berg, 1982). Conceivably, an αBgt effect was overlooked. Since only the proportion of cells displaying spontaneous synaptic events was scored in the presence and absence of toxin, a decrease in the mean amplitude of the depolarizations may have gone undetected. The fact that the number of αBgt-binding AChRs per ciliary ganglion is about 3-fold higher in situ than in culture (Corriveau and Berg, 1994) may have exacerbated the detection problem. An alternative possibility is that activation of perisynaptic AChRs requires a special synaptic configuration that only occurs when the pre- and postsynaptic neurons are properly matched. It is known that accessory oculomotor neurons, which provide the normal innervation of the ciliary ganglion, form morphologically distinct contacts on ciliary ganglion neurons in culture that are not found when ciliary ganglion neurons innervate each other (Fujii and Berg, 1987).

Though αBgt-sensitive receptors in situ produce much of the synaptic current observed in ciliary ganglion neurons, the receptors are not essential for generating action potentials in response to presynaptic stimulation. The high input resistance of the neurons enables the αBgt-resistant synaptic current unaided to elicit action potentials. Why would neurons maintain two classes of receptors for this purpose, each responding to the same transmitter from the same source? One possibility is that the two classes of receptors contribute differently under different stimulation paradigms: αBgt-sensitive AChRs with their rapid kinetics of activation and desensitization may be important for sustaining excitatory transmission at high frequencies. A different possibility is that each receptor subtype provides unique downstream effects through the second messenger cascade it activates (Vijayaraghavan et al., 1995). Even when the same second messenger is involved as in the case of calcium, it is clear that different cholinergic receptors on the neurons can achieve different effects in terms of the temporal and spatial patterns of calcium fluxes produced (Rathouz et al., 1995). If neurons can independently regulate the proportion of each receptor subtype functionally available, they could vary the kinds of secondary consequences achieved while sustaining excitatory transmission. This could provide a useful mechanism for manipulating the information content of synaptic signaling.

Experimental Procedures

Tissue Preparations

Ciliary ganglia with nerve roots attached were dissected from 13- to 14-day-old chick embryos and placed in a recording chamber with a volume of about 300 μl. The connective sheath covering the ganglion was softened by collagenase (10 mg/ml, type A, Boehringer Mannheim), and then removed with fine forceps. Part of the ganglion was further cleaned for 10–15 min with protease (5 mg/ml, type XIV, Sigma) applied with a glass pipette (20–40 μm opening) by gentle pressure. For whole-cell patch-clamp recording, the cells were viewed under Nomarski optics with a 40× objective (Zeiss, water immersion, NA 0.75). For intracellular recording with sharp electrodes, the cells were viewed with a dissecting microscope (Wild, model M5) at 40×. Ganglia were perfused at about 4 ml/min with normal Krebs solution containing 120 mM NaCl, 5 mM KCl, 1 mM NaH_2PO_4, 1 mM $MgSO_4$, 11 mM glucose, 25 mM NaHCO3, 2.5 mM $CaCl_2$, and gassed with 95% O_2 and 5% CO_2.

Whole-Cell Patch-Clamp Recording

Patch-clamp recording from neurons in intact ganglia was performed as previously described (Yawo and Chuhma, 1994). Patch pipettes were pulled from borosilicate glass (1.5 mm OD, Drummond Scientific). When filled with intracellular solution, the electrodes had resistance of 2–3 MΩ. Intracellular solution contained 140 mM CsCl, 2 mM MgATP, 0.2 mM GTP, 2 mM EGTA, 5 mM glucose, and 10 mM HEPES (pH 7.2). Omitting ATP and GTP from the recording solution did not affect the stability or time course of the synaptic currents. The series resistance had values of 4–8 MΩ; 80% compensation was applied during recording of evoked synaptic currents. The currents were elicited by stimulating the oculomotor nerve root with a suction pipette. Stimulations (10–300 ms, 10–100 V) were delivered with a Grass stimulator (model S88) at 20 or 30 s intervals unless otherwise indicated.

In some cells, regenerative Na^+ currents were observed, indicating insufficient series resistance compensation and space clamp. The Na^+ currents usually followed the peak of the evoked synaptic currents and had a faster time course; such cells were discarded. Some cells had synaptic currents larger than 8 nA but were excluded from the analysis because of the limitations of the space clamp. A few cells displayed a current reminiscent of a presynaptic action potential about 1 ms before the onset of the main synaptic event. The current was not blocked by 200 μM Cd^{2+} and was very likely the result of electrical coupling between the presynaptic terminal (calyx) and the ciliary neuron (Martin and Pilar, 1964; Dryer and Chiappinelli, 1985). Occasionally, recordings were obtained from calyces. In these cases, nerve stimulation produced a large inward current with little (<0.5 ms) or no delay between the end of stimulation and the onset of current.

Synaptic currents were recorded with an Axopatch-1C amplifier (Axon Instruments) on videotape (VR-10B, Instrutech). Data were filtered at 1 or 2 kHz (−3 dB, eight pole Bessel filter, Frequency Device) and digitized at 10 kHz (Digidata 1200, Axon Instruments). Analysis of evoked synaptic currents was performed with Axograph software (Axograph 2.0, Axon Instruments). Traces of four to five consecutive stimulations were averaged. The peak current amplitude was calculated by averaging three adjacent points at the peak. Decay time constants were obtained by fitting a 50 ms segment located after the peak with the method of maximum likelihood. In some cases, three exponentials provided a better fit of the decay phase of the evoked response than did two; this was also seen previously with responses from dissociated cells (Zhang et al., 1994). For compilation purposes, only the fast and slow time constants of decay were independently averaged for the evoked responses from all cells. Statistical analysis was performed with Statview software (version 4.01).

Spontaneous synaptic currents were recorded with patch electrodes coated with Sylgard. Data were filtered at 1 kHz and digitized continuously at 10 kHz with the Fetchex program (pClamp 5.0, Axon Instruments). Analysis of miniature currents was performed with a program written by P. Vincent (Vincent and Marty, 1993). For each event, the baseline level was calculated by averaging a segment of 90 (control) or 190 (αBgt-treated) points located immediately prior to the rising phase. The threshold of detection was set at about four times the baseline root-mean-square (rms) noise level. Each event was inspected visually to exclude false events such as large channel openings. The current amplitude was calculated by averaging four points at the peak.

ACh responses from dissociated cells were measured as previously described (Zhang et al., 1994). In brief, ciliary ganglia from 13- to 14-day-old chick embryos were dissociated, allowed to attach to the culture substratum, and then tested with whole-cell patch-clamp recording to quantify their responses to 0.5 and 2 mM ACh. Agonist was applied with a rapid delivery system (Zhang and Berg, 1995). The time of solution exchange by this method was under 2 ms as estimated from changes in the junction potential recorded from an open pipette. Usually both ACh concentrations were tested on the same cell, alternating the sequence of application. Solutions, procedures, and data analysis were as previously described (Zhang et al., 1994). Rise times and decay time constants were determined as described above for synaptic currents.

Intracellular Recording

For intracellular recording, sharp electrodes were filled with 2 M potassium acetate and had resistances of 35–80 MΩ. Membrane potentials were measured with an amplifier equipped with bridge circuit (WPI, model M701). The resting potential was determined upon withdrawal of the pipette at the end of each recording. Cells with resting potentials more positive than −60 mV were rejected. Data were analyzed with Axograph software.

Materials

White leghorn chick embryos were obtained locally and maintained at 37°C in a humidified incubator. αBgt was purchased from Biotoxins (St. Cloud, Florida); phospholine iodide (echothiophate) was purchased from Wyeth–Ayerst Laboratories, Incorporated. All other drugs were purchased from Sigma. Drugs dissolved in extracellular solution were applied by gravity from a set of reservoirs. This proved to be efficient for patch-clamp recordings, since all recordings were made from neurons lying on the surface of ganglion. In the case of intracellular recording, ganglia were incubated for over 1 hr before recording with 100 nM αBgt in Krebs solution gassed continuously with 95% O_2 and 5% CO_2. For control ganglia, the same procedure was applied in the absence of toxin. Ganglia were viable for as long as 5 hr under these conditions. All experiments were carried out at room temperature (20°C–23°C).

Acknowledgments

We thank P. Vincent for sharing his data analysis program. Grant support was provided by the National Institutes of Health (grant R01 NS12601), the Muscular Dystrophy Association, and the Council for Tobacco Research. Z.-w. Z. is an MDA Postdoctoral Fellow; J. S. C. is an NRSA Postdoctoral Fellow.

The costs of publication of this article were defrayed in part by the payment of page charges. This article must therefore be hereby marked *"advertisement"* in accordance with 18 USC Section 1734 solely to indicate this fact.

Received March 28, 1996; revised September 17, 1996.

References

Alkondon, M., and Albuquerque, E.X. (1993). Diversity of nicotinic acetylcholine receptors in rat hippocampal neurons. I. Pharmacological and functional evidence for distinct structural subtypes. J. Pharmacol. Exp. Ther. *265*, 1455–1473.

Atkins, P.W. (1986). Physical Chemistry, Third Edition (New York: Freeman).

Bertrand, D., Galzi, J.L., Devillers-Thiéry, A., Bertrand, S., and Changeux, J.P. (1993). Mutations at two distinct sites within the channel domain M2 alter calcium permeability of neuronal α7 nicotinic receptor. Proc. Natl. Acad. Sci. USA *90*, 6971–6975.

Chiappinelli, V.A. (1985). Actions of snake venom toxins on neuronal nicotinic receptors and other neuronal receptors. Pharmacol. Ther. *31*, 1–32.

Chiappinelli, V.A., and Giacobini, E. (1978). Time course of appearance of α-bungarotoxin binding sites during development of chick ciliary ganglion and iris. Neurochem. Res. *3,* 465–478.

Chiappinelli, V.A., and Zigmond, R.E. (1978). α-Bungarotoxin blocks nicotinic transmission in the avian ciliary ganglion. Proc. Natl. Acad. Sci. USA *75*, 2999–3003.

Chiappinelli, V.A., Cohen, J.B., and Zigmond, R.E. (1981). The effects of α- and β-neurotoxins from the venoms of various snakes on transmission in autonomic ganglia. Brain Res. *211*, 107–126.

Clarke, P., Quik, M., Adlkofer, F., and Thurau, K., eds. (1995). Advances in Pharmacological Sciences, Volume 2: Effects of Nicotine on Biological Systems (Basel, Switzerland: Birkhauser Verlag Press).

Clements, J.D. (1996). Transmitter timecourse in the synaptic cleft: its role in central synaptic function. Trends Neurosci. *19*, 163–171.

Corriveau, R.A., and Berg, D.K. (1994). Neurons in culture maintain acetylcholine receptor levels with far fewer transcripts than *in vivo*. J. Neurobiol. *25*, 1579–1592.

Couraud, J.Y., Koenig, H.L., and Di Giamberardino, L. (1980). Acetylcholinesterase molecular forms in chick ciliary ganglion: pre- and postsynaptic distribution derived from denervation, axotomy, and double section. J. Neurochem. *34*, 1209–1218.

Couturier, S., Bertrand, D., Matter, J.-M., Hernandez, M.-C., Bertrand, S., Millar, N., Valera, S., Barkas, T., and Ballivet, M. (1990). A neuronal nicotinic acetylcholine receptor subunit (α7) is developmentally regulated and forms a homo-oligomeric channel blocked by α-Btx. Neuron *5*, 847–856.

Dryer, S.E., and Chiappinelli, V.A. (1985). Properties of choroid and ciliary neurons in the avian ciliary ganglion and evidence for Substance P as a neurotransmitter. J. Neurosci. *5*, 2654–2661.

Fujii, J.T., and Berg, D.K. (1987). Formation of calyx-like contacts preferentially on appropriate target neurons in culture. Dev. Biol. *123,* 346–353.

Halvorsen, S.W., and Berg, D.K. (1987). Affinity labeling of neuronal acetylcholine receptor subunits with an α-neurotoxin that blocks receptor function. J. Neurosci. *7*, 2547–2555.

Jacob, M.H., and Berg, D.K. (1983). The ultrastructural localization of α-bungarotoxin binding sites in relation to synapses on chick ciliary ganglion neurons. J. Neurosci. *3*, 260–271.

Jacob, M.H., Berg, D.K., and Lindstrom, J.M. (1984). Shared antigenic determinant between the *Electrophorus* acetylcholine receptor and a synaptic component on chicken ciliary ganglion neurons. Proc. Natl. Acad. Sci. USA *81*, 3223–3227.

Kato, A.C., Vrachliotis, A., Fulpius, B., and Dunant, Y. (1980). Molecular forms of acetylcholinesterase in chick muscle and ciliary ganglion: embryonic tissues and cultured cells. Dev. Biol. *76,* 222–228.

Loring, R.H., and Zigmond, R.E. (1987). Ultrastructural distribution of ^{125}I-toxin F binding sites on chick ciliary neurons: synaptic localization of a toxin that blocks ganglionic nicotinic receptors. J. Neurosci. *7*, 2153–2162.

Loring, R.H., Chiappinelli, V.A., Zigmond, R.E., and Cohen, J.B. (1984). Characterization of a snake venom neurotoxin which blocks nicotinic transmission in the avian ciliary ganglion. Neuroscience *11*, 989–999.

Loring, R.H., Dahm, L.M., and Zigmond, R.E. (1985). Localization of α-bungarotoxin binding sites in the ciliary ganglion of the embryonic chick: an autoradiographic study at the light and electron microscopic level. Neuroscience *14*, 645–660.

Margiotta, J.F., and Berg, D.K. (1982). Functional synapses are established between ciliary ganglion neurones in dissociated cell culture. Nature *296*, 152–154.

Martin, A.R., and Pilar, G. (1964). An analysis of electrical coupling at synapses in the avian ciliary ganglion. J. Physiol. (Lond.) *171*, 454–475.

McGehee, D.S., and Role, L.W. (1995). Physiological diversity of nicotinic acetylcholine receptors expressed by vertebrate neurons. Annu. Rev. Physiol. *57*, 521–546.

McGehee, D., Heath, M., Gelber, S., and Role, L.W. (1995). Nicotine enhancement of fast excitatory synaptic transmission in CNS by presynaptic receptors. Science *269*, 1692–1697.

Olivieri-Sangiacomo, C., Del Fa, A., and Gangitano, C. (1983). Developmental distributive pattern of acetylcholinesterase in chick embryo ciliary ganglion. Brain Res. *283*, 61–69.

Picciotto, M.R., Zoli, M., Lena, C., Bessis, A., Lallemand, Y., LeNovere, N., Vincent, P., Pich, E.M., Brulet, P., and Changeux, J.-P. (1995). Abnormal avoidance learning in mice lacking functional high-affinity nicotine receptor in the brain. Nature *374*, 65–67.

Pugh, P.C., and Berg, D.K. (1994). Neuronal acetylcholine receptors that bind α-bungarotoxin mediate neurite retraction in a calcium-dependent manner. J. Neurosci. *14*, 889–896.

Pugh, P.C., Corriveau, R.A., Conroy, W.G., and Berg, D.K. (1995). A novel subpopulation of neuronal acetylcholine receptors among those binding α-bungarotoxin. Mol. Pharmacol. *47*, 717–725.

Radic, Z., Quinn, D.M., Vellom, D.C., Camp, S., and Taylor, P. (1995). Allosteric control of acetylcholinesterase catalysis by fasciculin. J. Biol. Chem. *270*, 20391–20399.

Rathouz, M.M., Vijayaraghavan, S., and Berg, D.K. (1995). Acetylcholine differentially affects intracellular calcium via nicotinic and muscarinic receptors on the same population of neurons. J. Biol. Chem. *270*, 14366–14375.

Ravdin, P.M., Nitkin, R.M., and Berg, D.K. (1981). Internalization of α-bungarotoxin on neurons induced by a neurotoxin that blocks neuronal acetylcholine sensitivity. J. Neurosci. *1*, 849–861.

Sargent, P.B. (1993). The diversity of neuronal nicotinic acetylcholine receptors. Annu. Rev. Neurosci. *16*, 403–443.

Scarsella, G., Toschi, G., Chiappinelli, V.A., and Giacobini, E. (1978). Molecular forms of acetylcholinesterase in the ciliary ganglion and iris of the chick: developmental changes and effects of axotomy. Dev. Neurosci. *1*, 133–141.

Schoepfer, R., Conroy, W.G., Whiting, P., Gore, M., and Lindstrom, J. (1990). Brain α-bungarotoxin binding protein cDNAs and MAbs reveal subtypes of this branch of the ligand-gated ion channel gene superfamily. Neuron *5*, 35–48.

Seguela, P., Wadiche, J., Dineley-Miller, K., Dani, J.A., and Patrick, J.W. (1993). Molecular cloning, functional properties, and distribution of rat brain α7: a nicotinic cation channel highly permeable to calcium. J. Neurosci. *13*, 596–604.

Smith, M.A., Stollberg, J., Lindstrom, J.M., and Berg, D.K. (1985). Characterization of a component in chick ciliary ganglia that cross-reacts with monoclonal antibodies to muscle and electric organ acetylcholine receptor. J. Neurosci. *5*, 2726–2731.

Ullian, E.M., and Sargent, P.B. (1995). Pronounced cellular diversity and extrasynaptic location of nicotinic acetylcholine receptor subunit immunoreactivities in the chicken pretectum. J. Neurosci. *15*, 7012–7023.

Vernallis, A.B., Conroy, W.G., and Berg, D.K. (1993). Neurons assemble acetylcholine receptors with as many as three kinds of subunits and can segregate subunits among receptor subtypes. Neuron *10*, 451–464.

Vijayaraghavan, S., Pugh, P.C., Zhang, Z.-w., Rathouz, M.M., and Berg, D.K. (1992). Nicotinic receptors that bind α-bungarotoxin on neurons raise intracellular free Ca^{2+}. Neuron *8*, 353–362.

Vijayaraghavan, S., Huang, B., Blumenthal, E.M., and Berg, D.K. (1995). Arachidonic acid as a possible negative feedback inhibitor of nicotinic acetylcholine receptors on neurons. J. Neurosci. *15*, 3679–3687.

Vincent, P., and Marty, A. (1993). Neighboring cerebellar Purkinje cells communicate via retrograde inhibition of common presynaptic interneurons. Neuron *11*, 885–893.

Wilson Horch, H.L., and Sargent, P.B. (1995). Perisynaptic surface distribution of multiple classes of nicotinic acetylcholine receptors on neurons in the chicken ciliary ganglion. J. Neurosci. *15*, 7778–7795.

Yawo, H., and Chuhma, N. (1994). ω-Conotoxin-sensitive and -resistant transmitter release from the chick ciliary presynaptic terminal. J. Physiol. (Lond.) *477*, 437–448.

Zhang, Z.-w., and Berg, D.K. (1995). Patch-clamp analysis of glycine-induced currents in chick ciliary ganglion neurons. J. Physiol. (Lond.) *487*, 395–405.

Zhang, Z.-w., Vijayaraghavan, S., and Berg, D.K. (1994). Neuronal acetylcholine receptors that bind α-bungarotoxin with high affinity function as ligand-gated ion channels. Neuron *12*, 167–177.

Zorumski, C.F., Thio, L.L., Isenberg, K.E., and Clifford, D.B. (1992). Nicotinic acetylcholine currents in cultured postnatal rat hippocampal neurons. Mol. Pharmacol. *41*, 931–936.